

Excited state dynamics of the Ho $3 +$ ions in holmium singly doped and holmium, praseodymium-codoped fluoride glasses

André Felipe Henriques Librantz, Stuart D. Jackson, Fabio Henrique Jagosich, Laércio Gomes, Gaël Poirier, Sidney José Lima Ribeiro, and Younes Messaddeq

Citation: *Journal of Applied Physics* **101**, 123111 (2007); doi: 10.1063/1.2749285

View online: <http://dx.doi.org/10.1063/1.2749285>

View Table of Contents: <http://scitation.aip.org/content/aip/journal/jap/101/12?ver=pdfcov>

Published by the [AIP Publishing](#)



Re-register for Table of Content Alerts

Create a profile.



Sign up today!



Excited state dynamics of the Ho^{3+} ions in holmium singly doped and holmium, praseodymium-codoped fluoride glasses

André Felipe Henriques Librantz

Center for Lasers and Applications, IPEN/CNEN-SP, P.O. Box 11049, São Paulo SP 05422-970, Brazil

Stuart D. Jackson^{a)}

Optical Fibre Technology Centre, The University of Sydney, 206 National Innovation Centre, Australian Technology Park, Eveleigh 1430, Australia

Fabio Henrique Jagosich and Laércio Gomes

Center for Lasers and Applications, IPEN/CNEN-SP, P.O. Box 11049, São Paulo SP 05422-970, Brazil

Gaël Poirier, Sidney José Lima Ribeiro, and Younes Messaddeq

Institute of Chemistry, UNESP, P.O. Box 355, Araraquara, São Paulo 14801-970, Brazil

(Received 29 September 2006; accepted 11 May 2007; published online 27 June 2007)

The deactivation of the two lowest excited states of Ho^{3+} was investigated in Ho^{3+} singly doped and Ho^{3+} , Pr^{3+} -codoped fluoride (ZBLAN) glasses. We establish that 0.1–0.3 mol % Pr^{3+} can efficiently deactivate the first excited (5I_7) state of Ho^{3+} while causing a small reduction of $\sim 40\%$ of the initial population of the second excited (5I_6) state. The net effect introduced by the Pr^{3+} ion deactivation of the Ho^{3+} ion is the fast recovery of the ground state of Ho^{3+} . The Burshtein model parameters relevant to the $\text{Ho}^{3+} \rightarrow \text{Pr}^{3+}$ energy transfer processes were determined using a least squares fit to the measured luminescence decay. The energy transfer upconversion and cross relaxation parameters for 1948, 1151, and 532 nm excitations of singly Ho^{3+} -doped ZBLAN were determined. Using the energy transfer rate parameters we determine from the measured luminescence, a rate equation model for 650 nm excitation of Ho^{3+} -doped and Ho^{3+} , Pr^{3+} -doped ZBLAN glasses was developed. The rate equations were solved numerically and the population inversion between the 5I_6 and the 5I_7 excited states of Ho^{3+} was calculated to examine the beneficial effects on the gain associated with Pr^{3+} codoping. © 2007 American Institute of Physics. [DOI: 10.1063/1.2749285]

I. INTRODUCTION

There has been a significant amount of interest for many decades in the use of sensitizing ions to transfer excitation energy from a pump source to an activator ion. There has been a similar amount of interest in the use of deactivator ions that receive excitation energy from the lower energy level of the luminescent transition of an activator ion; this interest has led to the improvement in several applications particularly in the area of material development for lasers and optical amplifiers. The luminescent 3F_4 level of Tm^{3+} , for example, can be efficiently depopulated by Ho^{3+} and Tb^{3+} ions in fluorozirconate (ZBLAN), tellurite, Ge–Ga–As–S–CsBr and $\text{GeO}_2\text{–Li}_2\text{O–K}_2\text{O–ZnO}$ codoped glasses, making these materials suitable for use as optical amplifiers operating in 1.4–1.5 μm region of the spectrum.^{1–5} For applications requiring laser operation at 2.9 μm , Ho^{3+} -doped LiYF_4 (YLF) crystal⁶ operating on the $^5I_6 \rightarrow ^5I_7$ transition has the potential for pulsed laser operation despite the longer ~ 16 ms lifetime of the lower laser (5I_7) level when compared to the lifetime of the upper laser (5I_6) level which is ~ 3 ms.⁷ Many applications, however, require continuous wave (cw) operation in this spectral range. To achieve this end, a deactivator ion must be introduced in order to quench the excited state population in the 5I_7 level. A 5I_7 level lifetime reduction to 2.2 ms in the presence of 1.2 mol % Nd^{3+}

in codoped YLF crystal⁷ has shown some promise, but the population of the upper 5I_6 laser level was reduced and the luminescence efficiency of the 2.9 μm emission decreased by approximately 50%.

Recently,⁸ it has been shown that effective deactivation of the 5I_7 level of Ho^{3+} using Pr^{3+} ions can lead to cw output from a ZBLAN-based fiber laser. With better choice of both the Ho^{3+} and Pr^{3+} ion concentrations, an unsaturated output power of 2.5 W was obtained from the fiber laser.⁹ This recent work extends past investigations^{10–12} into the successful use of the Pr^{3+} ion as a deactivator ion for the $^4I_{13/2}$ level of the $^4I_{11/2} \rightarrow ^4I_{13}$ laser transition of Er^{3+} -doped ZBLAN; the current output power of ~ 9 W from an Er^{3+} , Pr^{3+} -doped ZBLAN fiber laser demonstrates the power scaling potential of this particular rare-earth ion combination.¹³

In the present study we have carried out a detailed investigation of the luminescence emitted from the excited states of the Ho^{3+} ion in ZBLAN glass and in the presence of Pr^{3+} ions. We have determined the Burshtein model parameters for the luminescent decay and we have calculated the energy transfer rate parameters for the various energy transfer processes present in these glasses. We compare these results with other fluorescent systems involving deactivation and estimate the improvement in the performance of ZBLAN-based lasers operating at 2.9 μm . In light of potential directly diode pumped Ho^{3+} -doped ZBLAN fiber lasers, we numerically solved the rate equations for singly

^{a)}Electronic mail: s.jackson@ofc.usyd.edu.au

Ho^{3+} (4 mol %)-doped and Ho^{3+} (4 mol %), Pr^{3+} (x mol %)-codoped ZBLAN glasses under cw pumping at 655 nm to determine the population inversion and its dependence on the Pr^{3+} concentration.

II. EXPERIMENTAL PROCEDURE

The ZBLAN glasses were prepared as either single (Ho^{3+}) or double-doped (Ho^{3+} , Pr^{3+}) samples for the time-resolved luminescence spectroscopy experiments. The two sets of ZBLAN glasses were prepared from ultra-pure fluoride starting materials with the following compositions. (i) Ho^{3+} -doped samples: $(100-x) \times [53 \text{ ZrF}_4 - 20 \text{ BaF}_2 - 4 \text{ LaF}_3 - 20 \text{ NaF}] - x \text{ HoF}_3$ ($x = 2, 4, 6$ mol %). (ii) Ho^{3+} , Pr^{3+} -codoped samples which have the Ho^{3+} concentration constant at 4 mol %: $(96-y) \times [53 \text{ ZrF}_4 - 20 \text{ BaF}_2 - 4 \text{ LaF}_3 - 20 \text{ NaF}] - 4 \text{ HoF}_3 - y \text{ PrF}_3$ ($y = 0.1, 0.2, 0.3$ mol %).

The Ho^{3+} -doped ZBLAN and Ho^{3+} , Pr^{3+} -codoped ZBLAN glasses were produced by melting the starting materials at 850 °C for 120 min in a Pt–Au crucible. The liquids were poured into brass molds and annealed at 260 °C for 2 h to remove the mechanical stresses. The samples were cut and polished into $15 \times 10 \times 5$ mm³ pieces.

The absorption spectra of the glasses were measured using a spectrophotometer (Cary/OLIS 17D) operating in the range of 300–2000 nm. The lifetimes of the Ho^{3+} excited states, i.e., the 5I_6 and 5I_7 levels, were measured after pulsed laser excitation from a tunable optical parametric oscillator (OPO) that was pumped by the second harmonic of a Q-switched Nd:YAG (yttrium aluminum garnet) laser (Brilliant B from Quantel, France). Optical pulse widths of 4 ns at 1151 and 1948 nm were used to directly excite the 5I_6 and 5I_7 energy levels of Ho^{3+} , respectively. Selective optical excitation of the energy levels of Ho^{3+} was carried out in order to isolate the various components to the Ho^{3+} decay. The decay of the luminescence of the energy levels of Ho^{3+} was detected using an InSb infrared detector (Judson model J10D cooled to 77 K) in conjunction with a fast preamplifier (response time of ~ 0.5 μs) and analyzed using a digital 200 MHz oscilloscope (Tektronix TDS 410). All the fluorescence decay times were measured at 300 K. To isolate the luminescence signals, bandpass filters with $\sim 80\%$ transmission at 1200 and 2000 nm (each with a half width of 15 nm and an extinction coefficient outside this band of $\sim 10^{-5}$) were used.

III. EXPERIMENTAL RESULTS

A. Luminescence from the 5I_7 excited state of Ho^{3+}

The absorption spectrum of Ho^{3+} (4 mol %), Pr^{3+} (0.3 mol %)-doped ZBLAN glass is shown in Fig. 1. The spectrum was used to calculate the absorption cross section of the $^5I_8 \rightarrow ^5F_5$ absorption transition of Ho^{3+} at 650 nm in ZBLAN glass. The absorption spectrum of the Ho^{3+} and Pr^{3+} ions in ZBLAN codoped glass shows a strong overlap between the $^5I_8 \rightarrow ^5I_7$ absorption transition of Ho^{3+} (centered at 1950 nm) and the $^3H_4 \rightarrow ^3F_2$, 3H_6 absorption transition of

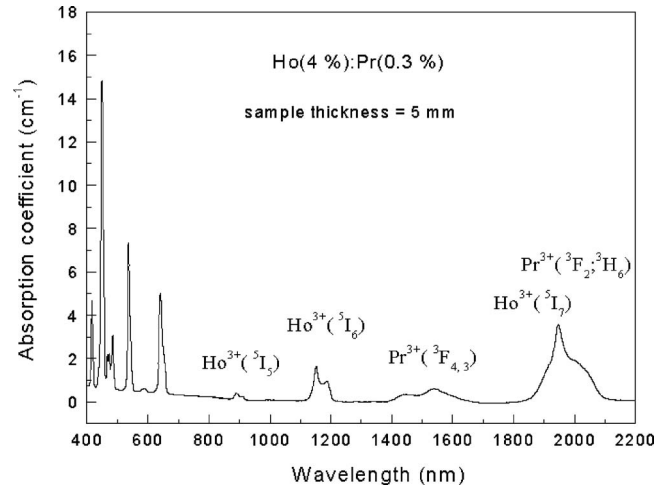


FIG. 1. Absorption spectrum of Ho^{3+} (4 mol %), Pr^{3+} (0.3 mol %)-doped ZBLAN glass measured at room temperature using the Cary 17D spectrophotometer. The sample thickness was equal to 5 mm. The Ho^{3+} ion concentration of 4 mol % corresponds to 5.5×10^{20} ions cm^{-3} .

Pr^{3+} (centered at 2100 nm); it is expected that efficient energy transfer will occur from the 5I_7 excited state of Ho^{3+} to the 3F_2 , 3H_6 states of Pr^{3+} .

Figure 2 shows the luminescence decay of the 5I_7 -excited state in Ho^{3+} (4 mol %)-doped ZBLAN and Ho^{3+} (4 mol %), Pr^{3+} (x mol %)-codoped ZBLAN glasses. It can be observed that a strong decrease in the 5I_7 excited state lifetime takes place for the Ho^{3+} (4 mol %), Pr^{3+} (0.2 mol %) and Ho^{3+} (4 mol %), Pr^{3+} (0.3 mol %)-codoped ZBLAN glasses in comparison with the decay of Ho^{3+} (4 mol %)-doped ZBLAN glass. The Ho^{3+} (5I_7) \rightarrow Pr^{3+} (3F_2 , 3H_6) nonradiative energy transfer (which we label ET1) is therefore very effective in Ho^{3+} , Pr^{3+} -codoped ZBLAN glass. The solid lines in Fig. 2 represent the best fit of the Ho^{3+} (5I_7) state luminescence decay using the Burshtein model,¹⁴ which

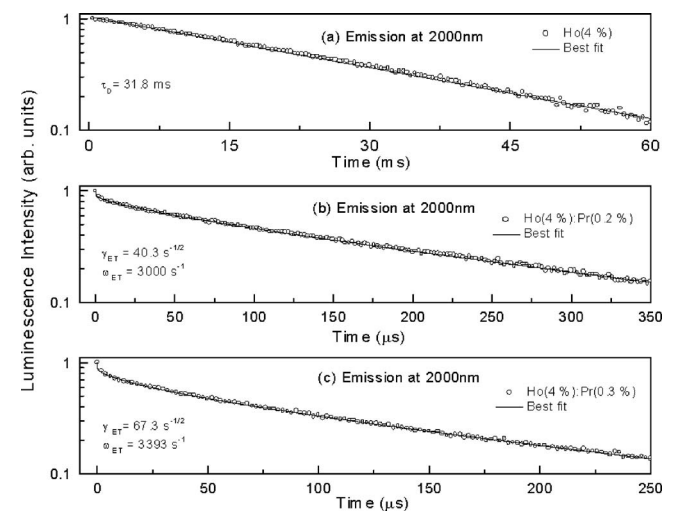


FIG. 2. Luminescence decay of the 5I_7 level of Ho^{3+} in (a) singly Ho^{3+} (4 mol %)-doped ZBLAN, (b) Ho^{3+} (4 mol %), Pr^{3+} (0.2 mol %)-codoped ZBLAN, and (c) Ho^{3+} (4 mol %), Pr^{3+} (0.3 mol %)-codoped ZBLAN induced by laser excitation at 1958 nm with a pulse duration of 4 ns and average energy of 5 mJ (and pulse repetition frequency of 10 Hz). The solid lines represent the best fit using the Burshtein model, and ω_{ET} and γ_{ET} are the derived energy transfer parameters using a least squares fit.

includes donor migration in the energy transfer process. The expression we used to fit the luminescence decay for a dipole-dipole interaction is given by¹⁴

$$I(t) = I_0 \exp\left(-\frac{t}{\tau_D} - \omega_{ET}t - \gamma_{ET}\sqrt{t}\right), \quad (1)$$

where τ_D ($=\tau_{D2}$) is equal to 31.8 ms and is the lifetime of 5I_7 level measured for Ho^{3+} (4 mol %)-doped ZBLAN. Note that this measured lifetime is longer than both the lifetime of the 5I_7 state measured in a low concentration system (12 ms for 0.1 mol % Ho^{3+}) and the radiative lifetime of 12.6 ms.¹⁵ This longer lifetime relates to the effects from excitation migration of the 5I_7 excited states at higher Ho^{3+} concentrations. γ_{ET} is the donor to acceptor (Pr^{3+}) energy transfer parameter and ω_{ET} is the transfer parameter which is related to the donor to acceptor energy transfer which is assisted by discrete excitation migration (or hopping) among donor (5I_7) states. The relative luminescence efficiency of the donor state (5I_7) can be calculated by integrating $I(t)$ for the entire decay. Integration of $I(t)$ has been used to calculate the effective lifetime of the ${}^3H_4(\text{Tm}^{3+})$ state due to $\text{Tm}^{3+}({}^3H_6)$, $\text{Tm}^{3+}({}^3H_4) \rightarrow \text{Tm}^{3+}({}^3F_4)$, $\text{Tm}^{3+}({}^3F_4)$ cross relaxation (CR) among Tm^{3+} ions in Yb^{3+} , Tm^{3+} -codoped systems.¹⁶ The relative luminescence efficiency (η_ℓ) has been calculated for the nonexponential decay of the donor state using the expression¹⁷

$$\eta_\ell = \frac{\int_0^\infty I(t)dt}{\int_0^\infty \exp(-t/\tau_D)dt} = \frac{\int_0^\infty I(t)dt}{\tau_D}. \quad (2)$$

In Eq. (2) we have used the normalized luminescence decay $I(t)$ such that $I(0)=I_0=1$, where I_0 is the fluorescence intensity at $t=0$ and $I(t \rightarrow \infty)=0$. Using $\eta_\ell = W_D/(W_D+W_{ET})$, where $W_D = \tau_D^{-1}$ is the donor intrinsic decay rate parameter and W_{ET} is the donor to acceptor energy transfer rate parameter, one can obtain

$$W_{ET} = \frac{1}{\tau_D} \left(\frac{1 - \eta_\ell}{\eta_\ell} \right). \quad (3)$$

In Eq. (3) $W_{ET}=0$ when $\eta_\ell=1$ and $W_{ET} \rightarrow \infty$ for $\eta_\ell \rightarrow 0$, as expected. The $\text{Ho}^{3+} \rightarrow \text{Pr}^{3+}$ transfer rate parameter for ET1 (i.e., $W_{ET}=W_{ET1}$) was calculated using Eq. (3) that incorporates the relative luminescence efficiency of the 5I_7 (Ho^{3+}) state and the intrinsic lifetime of this level ($\tau_D = \tau_{D2} = 31.8$ ms). The values of W_{ET1} are given in Table I.

Based on this result, we can establish that the decay of the 5I_7 state is practically totally radiative in ZBLAN glass and the nonradiative multiphonon decay rate to the ground state is negligible if these measurements are performed at room temperature. The relative luminescence efficiencies of the two lowest excited states of Ho^{3+} were obtained using the relation $\eta_\ell = \int_0^\infty I_i(t)dt / \tau_{Di}$, where $i=2$ refers to the 5I_7 level and $i=3$ to the 5I_6 state. Table I gives the energy transfer parameters (ω_{ET} , γ_{ET}) and the luminescence efficiency (η_ℓ) of 5I_7 state, which was diminished by ET1. One may obtain

TABLE I. Energy transfer parameters relating to the 5I_7 level. The energy transfer parameters were obtained from the best fit to the 2000 nm luminescence of ZBLAN glasses double doped with 4 mol % Ho^{3+} and 0.1, 0.2, or 0.3 mol % Pr^{3+} . The energy transfer parameters γ_{ET} and ω_{ET} were obtained using a least squares fit and $\tau_{D2}=31.8$ ms, which was measured independently from a Ho^{3+} (4 mol %)-doped ZBLAN sample. The relative luminescence efficiency η_ℓ was calculated using the integration of the normalized luminescence decay of Ho^{3+} in Ho^{3+} , Pr^{3+} -codoped ZBLAN.

Luminescence from the 5I_7 level of Ho^{3+}				
Pr^{3+} (mol %)	C_{DA} ($\text{cm}^6 \text{s}^{-1}$) (10^{-38})	γ_{ET} ($\text{s}^{-1/2}$)	ω_{ET} (s^{-1})	η_ℓ
0.1	3.1 ± 0.4	18.1 ± 0.6	1455 ± 3	1.428×10^{-2}
0.2	3.9 ± 0.7	40.3 ± 0.8	3000 ± 6	5.723×10^{-3}
0.3	4.8 ± 0.7	67.3 ± 1.1	3393 ± 27	3.773×10^{-3}
Migration assisted $\text{Ho}^{3+}({}^5I_7) \rightarrow \text{Pr}^{3+}$				
Pr^{3+} (mol %)	W_{ET1} (s^{-1})	γ_{ET}^2 (s^{-1})	R ($=\gamma_{ET}^2/W_{ET1}$)	
0.1	2171	328	0.15	
0.2	5463	1624	0.30	
0.3	8302	4529	0.55	

the microscopic transfer constant $C_{DA}(\text{cm}^6 \text{s}^{-1})$ using the following expression that relates this constant with the energy transfer parameter $\gamma_{ET}(\text{s}^{-1/2})$,

$$C_{DA} = \frac{9\gamma_{ET}^2}{16\pi^3 c_A^2}, \quad (4)$$

where c_A is the Pr^{3+} concentration. The calculated values of C_{DA} varied from 3.1×10^{-38} to $4.8 \times 10^{-38} \text{cm}^6 \text{s}^{-1}$ as the Pr^{3+} concentration changed from 0.1 to 0.3 mol %, as shown in Table I. The average value of C_{DA} for ET1 obtained in this work was equal to $3.9 \times 10^{-38} \text{cm}^6 \text{s}^{-1}$, which is higher than the microscopic rate constant found in the case of $\text{Ho}^{3+}({}^5I_7)$ deactivation by Nd^{3+} ions in $\text{Ho}:\text{Nd}:\text{YLF}$ crystal in which case C_{DA} was $8.6 \times 10^{-41} \text{cm}^6 \text{s}^{-1}$.⁷

If one assumes that γ_{ET}^2 relates to direct energy transfer, one can calculate the ratio $R = \gamma_{ET}^2/W_{ET}$, which determines the relative contribution of direct energy transfer to the total energy transfer. Table I shows that the contribution of the direct energy transfer to the total energy transfer increases (i.e., $R=0.15 \rightarrow 0.55$) and the influence of energy migration among donor ions decreases with increasing Pr^{3+} concentration. This situation is expected because with increasing Pr^{3+} concentration each Ho^{3+} excitation finds a Pr^{3+} ion faster, i.e., less energy migration among Ho^{3+} ions is necessary before direct energy transfer to a Pr^{3+} ion takes place.

B. Luminescence from the 5I_6 excited state of Ho^{3+}

Figure 3 shows the luminescence decay of the 5I_6 excited state of Ho^{3+} observed at 1200 nm due to the $\text{Ho}^{3+}({}^5I_6) \rightarrow \text{Pr}^{3+}({}^3F_5, {}^3F_4)$, energy transfer process (which we label ET2) in Ho^{3+} , Pr^{3+} -codoped ZBLAN glass. The solid line in Figs. 3(a) and 3(b) represents the best fit to the luminescence decay using the Burshtein model, i.e., Eq. (1). The energy transfer rate parameter of ET2 with $W_{ET}=W_{ET2}$ was calculated using Eqs. (2) and (3), where η_ℓ is now the relative luminescence efficiency of the 5I_6 excited state and

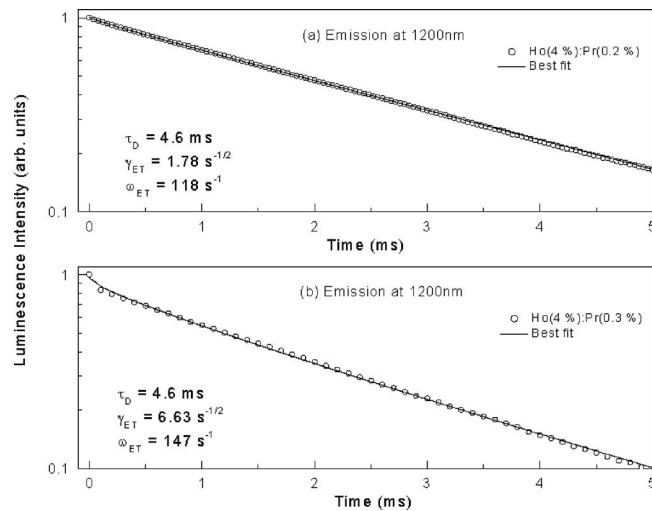


FIG. 3. Luminescence decay of the 5I_6 level of (a) Ho^{3+} (4 mol %), Pr^{3+} (0.2 mol %)-co doped ZBLAN and (b) Ho^{3+} (4 mol %), Pr^{3+} (0.3 mol %)-co doped ZBLAN. The 1200 nm luminescence was produced by a pulsed laser excitation at 1151 nm with a pulse duration of 4 ns and mean energy of 6 mJ at 10 Hz. The solid lines represent the best fit using the Burshtein model, and ω_{ET} and γ_{ET} are the derived energy transfer parameters using a least squares fit.

$\tau_D = \tau_{D3} = 4.6$ ms. The values of $W_{\text{ET}2}$ and γ_{ET}^2 are given in Table II. The values of R shown in Table II show that in a similar manner to ET1 the influence of direct energy transfer increases (i.e., $R = 0.009 \rightarrow 0.15$) and the influence of energy migration among donor ions decreases with increasing Pr^{3+} concentration. The ratio of direct energy transfer to the total energy transfer is smaller for ET2 compared to ET1, which suggests that more energy migration is required for ET2 compared to ET1.

Table II gives the energy transfer parameters (ω_{ET} , γ_{ET}) and the relative luminescence efficiency (η_ℓ) of the 5I_6 state due to ET2. The microscopic transfer constant C_{DA} varies from 0.18×10^{-41} to 3.51×10^{-41} $\text{cm}^6 \text{s}^{-1}$ in the case of the

TABLE II. Energy transfer parameters relating to the 5I_6 level. The energy transfer parameters were obtained from the best fit to the 1200 nm luminescence of ZBLAN glasses double doped with 4 mol % Ho^{3+} and 0.1, 0.2, or 0.3 mol % Pr^{3+} . The energy transfer parameters γ_{ET} and ω_{ET} were obtained using a least squares fit and $\tau_{D2} = 4.6$ ms, which was measured independently from a Ho^{3+} (4 mol %)-doped ZBLAN sample. The relative luminescence efficiency η_ℓ was calculated using the integration of the normalized luminescence decay of Ho^{3+} in Ho^{3+} , Pr^{3+} -doped ZBLAN.

Pr^{3+} (mol %)	Luminescence from the 5I_6 level of Ho^{3+}			
	C_{DA} ($\text{cm}^6 \text{s}^{-1}$) (10^{-40})	γ_{ET} ($\text{s}^{-1/2}$)	ω_{ET} (s^{-1})	η_ℓ
0.1	0.69 ± 0.08	0.85 ± 0.05	67.0 ± 0.1	0.7285
0.2	0.76 ± 0.06	1.78 ± 0.06	118.0 ± 0.3	0.5949
0.3	4.69 ± 0.29	6.63 ± 0.21	147.0 ± 1.2	0.4433
Pr^{3+} (mol %)	Migration assisted $\text{Ho}^{3+}(^5I_6) \rightarrow \text{Pr}^{3+}$ energy transfer			
	$W_{\text{ET}2}$ (s^{-1})	γ_{ET}^2 (s^{-1})	R ($= \gamma_{\text{ET}}^2 / W_{\text{ET}2}$)	
0.1	81	0.73	0.009	
0.2	148	3.2	0.021	
0.3	273	44	0.161	

Ho^{3+} (5I_6) deactivation by the Pr^{3+} ($^3F_4, ^3F_3$) states, when the Pr^{3+} concentration changes from 0.1 to 0.3 mol %. The average value of C_{DA} for ET2 is 2.05×10^{-41} $\text{cm}^6 \text{s}^{-1}$ is three order of magnitude smaller than the C_{DA} value for ET1 and is approximately 36 times bigger than the corresponding parameter determined for the case of Ho^{3+} (5I_6) deactivation by Nd^{3+} in $\text{Ho}:\text{Nd}:\text{YLF}$ crystal ($C_{\text{DA}} = 5.6 \times 10^{-42}$ $\text{cm}^6 \text{s}^{-1}$).⁷ This indicates that the deactivation of the Ho^{3+} (5I_6) state by energy transfer to Pr^{3+} ions will potentially have a larger impact on the population inversion of the 2.9 μm laser transition compared to deactivation of the Ho^{3+} (6I_6) state that would be introduced by Nd^{3+} ions.

C. Energy transfer upconversion (ETU) from the lowest excited states of Ho^{3+}

Two emission bands centered at 1200 and 655 nm were observed in Ho^{3+} (4 mol %) -doped ZBLAN produced by pulsed laser excitations at 1958 and 1151 nm, respectively. The temporal characteristics of both upconversion emissions were observed to be dependent on the excitation energy density up to the limit of ~ 0.2 J/cm^3 . For larger energy densities we observed a constant upconversion transient response. (The excitation energy densities were determined for constant energies of 3.1 mJ at 1958 nm and 8 and 12 mJ at 1151 nm. Four focus positions provided excitation volumes of 3.9×10^{-3} , 7.6×10^{-3} , 15.7×10^{-3} , and 35.3×10^{-3} cm^3 .) This observation cannot be applied to the luminescence decay of the lower excited (or donor) level involved in the upconversion process because one finds that the initial part of the decay curve of the donor level changes its slope as the pulse energy is varied. When we measured the intrinsic 5I_7 and 5I_6 fluorescence decays, we used a 6 mJ pulse energy (i.e., 1.9 mJ absorbed) to minimize the effects from ETU. This is demonstrated by the fact that the best fit of the 5I_7 (and 5I_6) luminescence decay curve is purely exponential, as seen in Fig. 2(a). The upconversion luminescence at 1200 nm was produced by a phonon-assisted ETU process, which we label ETU1 that can be represented by $\text{Ho}^{3+}(^5I_7, ^5I_7) \rightarrow \text{Ho}^{3+}(^5I_6, ^5I_8)$. Figure. 4 displays the 1200 nm luminescence decay of 5I_6 level when directly excited at 1151 nm [Fig. 4(a)] and when indirectly excited at 1958 nm by the ETU1 process [Fig. 4(b)].

A second upconversion luminescence at 655 nm was produced after two interacting 5I_6 states promote excitation to the 5F_5 level by way of a similar ETU process, labeled here as ETU2 and which can be represented by $\text{Ho}^{3+}(^5I_6, ^5I_6) \rightarrow \text{Ho}^{3+}(^5F_5, ^5I_8)$. Figures 5(a) and 5(b) show the luminescence transient measured at 655 nm from the Ho^{3+} (5F_5) excited state of Ho^{3+} (4 mol %)-doped ZBLAN. This 655 nm luminescence was produced by two distinct ways using (i) excitation at 532 nm to produce the $^5I_8 \rightarrow ^5S_2$ absorption transition which was followed by fast (~ 20 μs) decay to 5F_5 state, see Fig. 5(a); (ii) indirect excitation at 1151 nm to produce the $^5I_8 \rightarrow ^5I_6$ absorption transition which was followed by ETU2, see Fig. 5(b). Despite the fact that 655 nm upconversion luminescence has also been observed in Ho^{3+} , Pr^{3+} -codoped ZBLAN, we measured the ETU2 rate parameter using singly Ho^{3+} -doped ZBLAN in

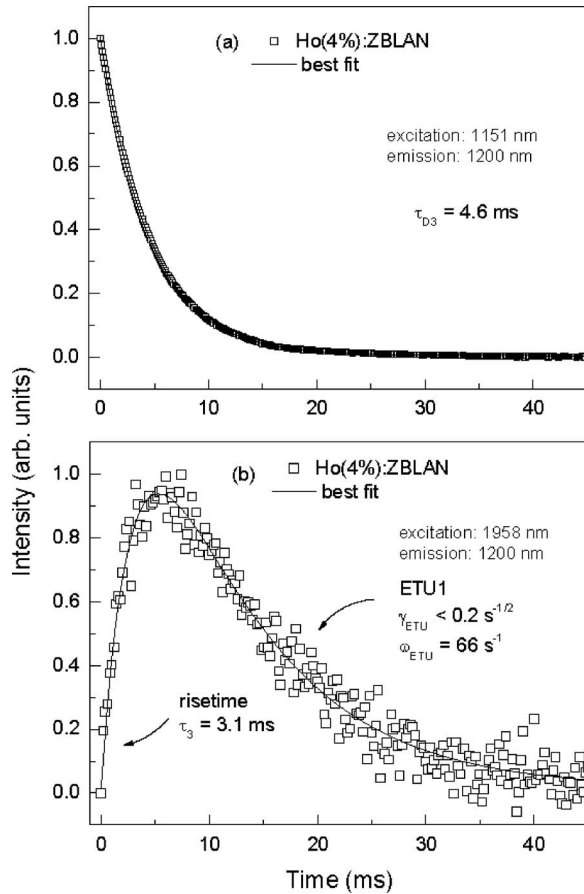


FIG. 4. (a) Luminescence decay of the 5I_6 excited state at 1200 nm measured after pulsed laser excitation at 1151 nm in singly Ho^{3+} (4 mol %)-doped ZBLAN (density of excited 5I_7 states of $\sim 5 \times 10^{17} \text{ cm}^{-3}$) and (b) the upconversion luminescence at 1200 nm induced by pulsed laser excitation at a wavelength of 1958 nm (pulse energy=3.1 mJ in 4 ns) having a density of excited (5I_7) states of $1.56 \times 10^{18} \text{ cm}^{-3}$. The solid line represents the best fit using the Burshtein model, and ω_{ETU} and γ_{ETU} are the ETU1 parameters using a least squares fit.

order to eliminate the influence of ET2. The solid lines in Figs. 4(b) and 5(b) represent the best fit to the 1200 and 655 nm emissions using Eq. (5) that has been derived for the acceptor luminescence transient where the energy transfer involves the Burshtein (or Inokuti-Hirayama) model for a dipole-dipole energy transfer.¹⁸ The relation is given by

$$I = I_0 \left[\exp\left(-\frac{t}{\tau_D} - \omega_{\text{ETU}}t - \gamma_{\text{ETU}}\sqrt{t}\right) - \exp\left(-\frac{t}{\tau_A}\right) \right], \quad (5)$$

where τ_A is the total lifetime of the acceptor excited state and τ_D is the intrinsic lifetime of the donor excited (Ho^{3+}) ion. The first term in Eq. (5) gives the nonexponential decay of the donor excited state directly involved in the ETU process. The second term is the acceptor excited state decay. The adjustable transfer parameters ($\omega_{\text{ETU1}}, \gamma_{\text{ETU1}}$) and ($\omega_{\text{ETU2}}, \gamma_{\text{ETU2}}$) in Eq. (5) relate to ETU1 and ETU2 processes, respectively. The best fit to the upconversion luminescence gave (a) $\omega_{\text{ETU1}} = 66 \text{ s}^{-1}$ and $\gamma_{\text{ETU1}} < 0.2 \text{ s}^{-1/2}$ for 1200 nm emission; (b) $\omega_{\text{ETU2}} = 33 \text{ s}^{-1}$ and $\gamma_{\text{ETU2}} = 22 \text{ s}^{-1/2}$ for 655 nm emission, measured for Ho^{3+} (4 mol %)-doped ZBLAN. The luminescence efficiency of the donors in the

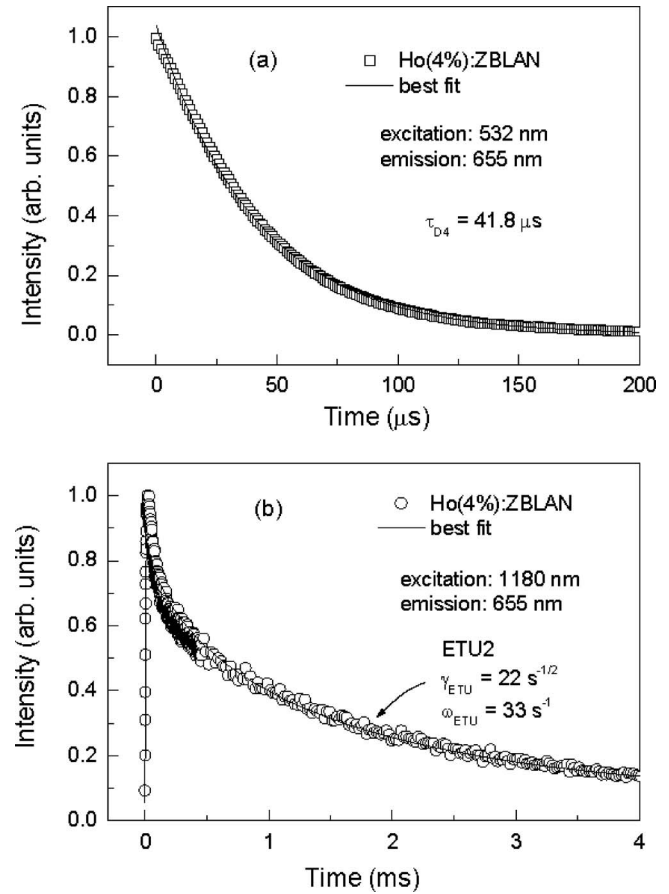


FIG. 5. The 5F_5 excited state luminescence of Ho^{3+} observed at 655 nm in singly Ho^{3+} (4 mol %)-doped ZBLAN glass after (a) direct excitation at 532 nm and (b) exciting the 5I_6 state at a wavelength of 1151 nm (pulse energy=8 mJ in 4 ns) having a density of excited (5I_6) states of $1.17 \times 10^{18} \text{ cm}^{-3}$. The solid line represents the best fit using the Burshtein model, and ω_{ETU} and γ_{ETU} are the ETU2 parameters using a least squares fit.

lower state that are involved in the ETU process was obtained using the following expression:

$$\eta_\ell = \frac{1}{\tau_D} \int_0^\infty \exp\left(-\frac{t}{\tau_D} - \omega_{\text{ETU}}t - \gamma_{\text{ETU}}\sqrt{t}\right) dt, \quad (6)$$

in which $I_0 = 1$ for $t = 0$, according to Eq. (2). The ETU rate parameter (W_{ETU}) was obtained using an expression similar to Eq. (3). The relative luminescence efficiencies (η_ℓ) due to ETU1 and ETU2 were obtained using $\tau_D(^5I_7) = 31.8 \text{ ms}$ and $\tau_D(^5I_6) = 4.6 \text{ ms}$ in Eq. (6). The ETU rate parameters W_{ETU1} and W_{ETU2} were obtained for the Ho^{3+} -doped ZBLAN system, using an equation similar to Eq. (3). By observing the 655 nm luminescence transient shown in Fig. 5(b), one observes that the fluorescence decay is consistent with the measured mean decay time (τ) of the donor (5I_6) state involved in the ETU2 process ($\tau = 1.33 \text{ ms}$). On the other hand, the 655 nm luminescence has a short decay time of $\sim 41.8 \mu\text{s}$ when this level is directly excited at 532 nm by the short laser pulse of 4 ns duration and a pulse energy of 5 mJ, as shown in Fig. 5(a) for the Ho^{3+} (4 mol %)-doped ZBLAN glass. The 655 nm emission exhibits the shortened decay time of 42 μs compared to the intrinsic 290 μs due to the phonon-assisted CR interaction $\text{Ho}^{3+} (^5F_5, ^5I_6) \rightarrow \text{Ho}^{3+} (^5I_8, ^5I_7)$ that depopulates this state in a highly con-

TABLE III. Parameters used in the rate equation modeling.

Luminescence branching ratio and radiative lifetimes of Ho ³⁺ ^a				
Transition	β	τ_R	τ (expt)	W_{nr} (s ⁻¹)
⁵ F ₅ →		500 μs	290 μs	1448
⁵ I ₆	0.05			
⁵ I ₇	0.18			
⁵ I ₈	0.77			
⁵ I ₆ →		5.9 ms	3.5 ms	116.2
⁵ I ₇	0.09			
⁵ I ₈	0.91			
⁵ I ₇ → ⁵ I ₈	1	12.6 ms	12 ms	
Ho ³⁺ →Ho ³⁺ energy transfer rate parameters (expt) ^b				
Ho ³⁺ (mol %)	W_{CR} (s ⁻¹)	$\eta_l(^5F_5)$		
2	107 76	0.2424		
4	194 87	0.1503		
6	251 23	0.1207		
Ho ³⁺ →Pr ³⁺ energy transfer rate parameters (expt) ^b				
Pr ³⁺ (mol %)	W_{ET1} (s ⁻¹)	W_{ET2} (s ⁻¹)	$\eta_l(^5I_7)$	$\eta_l(^5I_6)$
0.1	2171	81	1.427×10^{-2}	0.7285
0.2	5463	148	5.723×10^{-3}	0.5949
0.3	8302	273	3.773×10^{-3}	0.4433

^aValues obtained from the literature (Ref. 15).^bExperimental relative luminescence efficiencies and calculated rate values (this work).

concentrated system, i.e., for $[\text{Ho}^{3+}] > 0.5$ mol %. The luminescence decay of the ⁵F₅-excited state was measured for three Ho³⁺-doped ZBLAN samples (2, 4, and 6 mol %) by direct excitation at 532 nm. The relative luminescence efficiency of the ⁵F₅ state was obtained for the three Ho³⁺-doped ZBLAN samples using the integration of the luminescence decay curve previously described by Eq. (2). The values obtained are given in Table III as well the corresponding CR rate parameter W_{CR} that was calculated using a similar equation to Eq. (3) with $\tau_D = \tau_{D4} = 290$ μs. The calculated values are given in Table III.

D. Model for ETU in Ho³⁺-doped ZBLAN

A detailed investigation of the time dependence of the ETU luminescence transient was carried out by monitoring the upconverted luminescence at 1200 and 655 nm as a function of the absorbed excitation energy density and hence the density of excited Ho³⁺ ions. We made a fit to the luminescence transient using the Burshtein model given by Eq. (5) for a dipole-dipole interaction. The rate parameters for ETU were obtained using the integration method given by Eq. (6) and a similar equation to Eq. (3). The results are presented in Table IV. Figures 6(a) and 6(b) display the ETU rate parameters for ETU2 and ETU1 as a function of the density of excited Ho³⁺ ions. It can be observed that the rate parameter of both ETU processes reaches a constant rate when the excited Ho³⁺ ion density reaches a value of 2×10^{18} cm⁻³; this behavior suggests that there exists a critical distance R_C between excited Ho³⁺ ions for both ETU processes. Based on a statistically random separation between the excited Ho³⁺ ions in the glass lattice, we can say that the fraction of excited

TABLE IV. Parameters relating to the proposed model for the ETU processes observed in Ho³⁺(4 mol %)-doped ZBLAN.

	Ho ³⁺ →Ho ³⁺ ETU rate parameters (expt)	
	ETU1	ETU2
K_0 (s ⁻¹)	72	650
N_C (cm ⁻³)	3.6×10^{17}	2.94×10^{17}
R_C (Å)	87	70

Ho³⁺ ions fdR , which have another excited Ho³⁺ ion as the closest neighbor between distance R and $R+dR$, is given by,¹⁹

$$fdR = 4\pi R^2 N_{\text{Ho}} \frac{N^*}{N_{\text{Ho}}} \left(1 - \frac{N^*}{N_{\text{Ho}}}\right)^{[\pi 3R^3 N_{\text{Ho}} - 2]} dR, \quad (7)$$

where N^* is the concentration of Ho³⁺ excited ions (cm⁻³) and N_C is the critical concentration of excited Ho³⁺ ions which is related to R_C . Integrating Eq. (7) between R_m (the minimum distance between Ho³⁺ ions) and $R=\infty$ yields the ETU efficiency as a function of N^* according to

$$\eta_{\text{ETU}} = \int_{R_m}^{R_C} fdR \times 1 + \int_{R_C}^{\infty} fdR \times 0 = 1 - \exp(-N_C/N^*), \quad (8)$$

where we use $\int_{R_C}^{\infty} fdR = \exp(-N_C/N^*)$, which has been determined previously.¹⁹ The observation that the ETU rate pa-

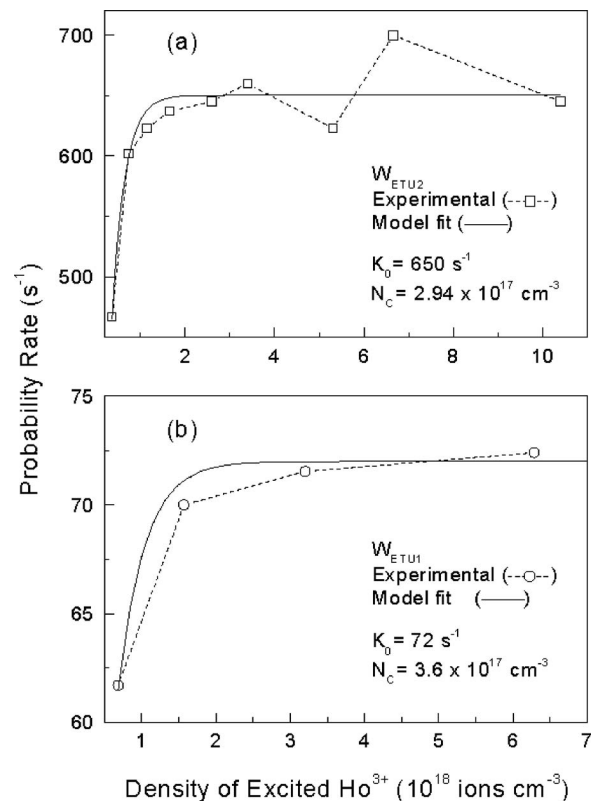


FIG. 6. ETU rate parameter as a function of the experimental excited Ho³⁺ ion density (N^*) obtained by measuring the luminescence transient of (a) the ⁵F₅ level after excitation at 1151 nm and (b) the ⁵I₆ level after excitation at 1958 nm. The solid lines represent the best fit using the proposed model for ETU.

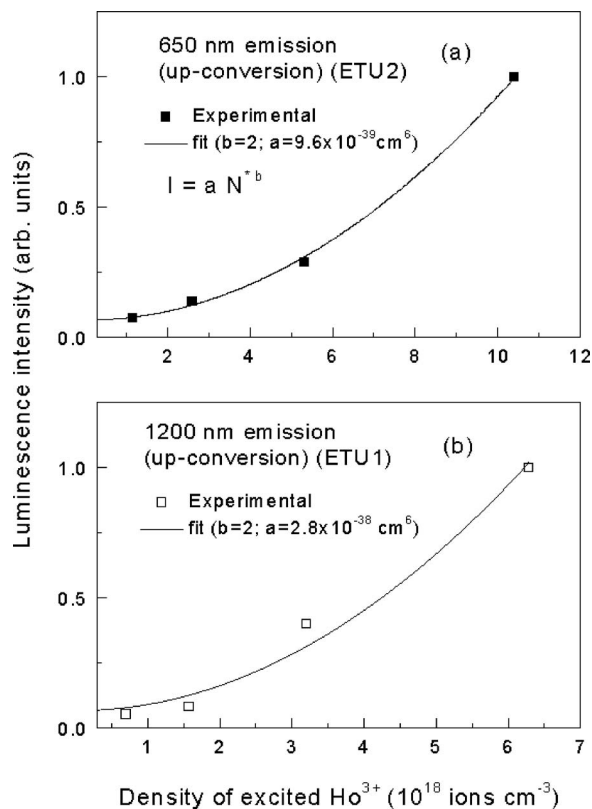


FIG. 7. Measured dependence of (a) 650 nm and (b) 1200 nm emission as a function of the excited Ho^{3+} ion density. The solid line represents $I = aN^{*b}$, where $b=2$ for both ETU processes.

parameter dependence on N^* in Figs. 6(a) and 6(b) displays a constant probability rate for higher excitation densities indicates that the ETU relative efficiency for large values of N^* should be given by $\eta_{\text{ETU}}(N^*) = W_{\text{ETU}}/K_0$, where K_0 is the rate parameter constant. The solid lines in Figs. 6(a) and 6(b) represent the best fit using the model, which gave $N_C = 2.94 \times 10^{17} \text{ cm}^{-3}$ and $K_0 = 650 \text{ s}^{-1}$ for ETU2 and $N_C = 3.6 \times 10^{17} \text{ cm}^{-3}$ and $K_0 = 72 \text{ s}^{-1}$ for ETU1. These values for K_0 should be used in a rate equation system simulating the operation of a laser because under these circumstances, higher excited Ho^{3+} ion densities ($N^* \sim 10^{19} \text{ cm}^{-3}$) are usually present.

The luminescence intensities at 1200 and 655 nm produced by the ETU1 and ETU2 processes, respectively as a function of the excited Ho^{3+} density are presented in Figs. 7(a) and 7(b). It can be observed that the emissions are dependent on the square of N^* , as represented by the solid and open squares in Figs. 7(a) and 7(b). The proposed model for ETU predicts an ETU rate linearly dependent on the N^* for $N^* \ll N_C$, i.e., $W_{\text{ETU}} \propto N^*$, as has been previously reported for ETU process between two Nd^{3+} ions in the ${}^4F_{3/2}$ state.²⁰

IV. DISCUSSION

The rate parameters for ETU1 correspond to 11% of the rate parameters for ETU2, consequently ETU does not favor a population inversion between the 5I_6 and 5I_7 energy levels in singly Ho^{3+} -doped ZBLAN glass. The opposite situation has been observed in the case of Er^{3+} -doped ZBLAN glass, where the corresponding rate parameter values for ETU1 are

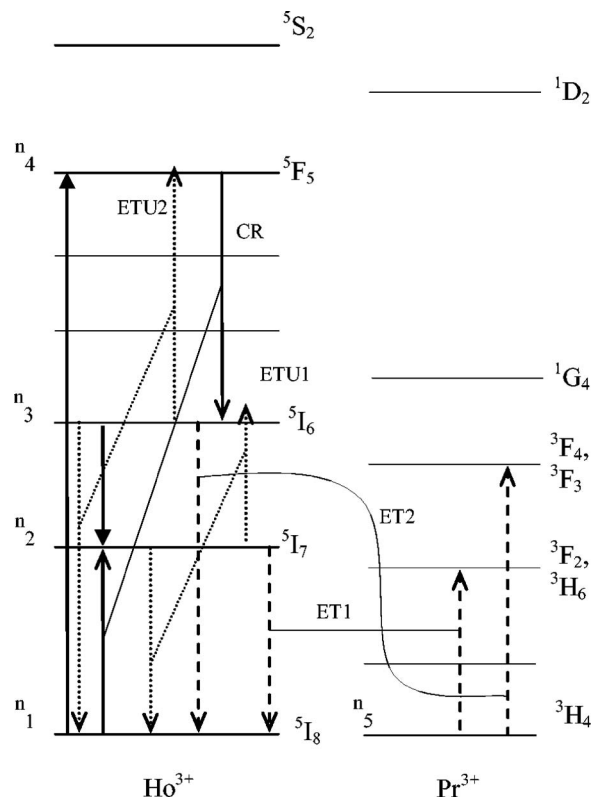


FIG. 8. Simplified energy level diagram for the Ho^{3+} , Pr^{3+} system used for the rate equations modeling. The diagram shows the optical pumping at 650 nm, the 2900 nm laser emission from the 5I_6 excited state of Ho^{3+} , and the $\text{Ho}^{3+} \rightarrow \text{Pr}^{3+}$ energy transfer processes.

three times larger than the corresponding rate parameter values for ETU2 and ETU contributes positively to a population inversion.²¹ (The ETU processes in Er^{3+} involve similarly positioned energy levels as in Ho^{3+} .) The ET1 energy transfer process has a larger rate parameter than the ETU2 process in Ho^{3+} (4 mol %), Pr^{3+} (0.3 mol %)-doped ZBLAN, which will minimize the negative effect of ETU on the laser gain. ET1 effectively quenches the 5I_7 intrinsic lifetime of 31.8 ms to such an extent that the mean decay time is only 120 μs for Ho^{3+} (4 mol %), Pr^{3+} (0.3 mol %)-codoped ZBLAN glass. Similar effects have been observed on the lower laser level of Er^{3+} (8.75 mol %), Pr^{3+} (1.55 mol %)-codoped ZBLAN glass, where the Er^{3+} (${}^4I_{13/2}$) intrinsic lifetime of 9 ms is reduced to 20 μs due an efficient $\text{Er}^{3+}({}^4I_{13/2}) \rightarrow \text{Pr}^{3+}({}^3F_3, {}^3F_4)$ energy transfer process.²¹

A. Rate equations for the Ho^{3+} , Pr^{3+} -codoped ZBLAN system

Figure 8 shows a simplified energy level scheme of the Ho^{3+} , Pr^{3+} system considered for cw diode laser pumping at 650 nm. n_1 , n_2 , n_3 , and n_4 are the 5I_8 , 5I_7 , 5I_6 , and 5F_5 populations of Ho^{3+} , respectively. For the Pr^{3+} ion, only the ground state 3H_4 (n_5) population was considered because the 3F_4 , 3F_3 , 3F_2 , 3H_6 , and 3H_5 excited state populations of Pr^{3+} are strongly depopulated by fast multiphonon decay to the ground state and consequently they were neglected in the

model. The rate equations comprising the model using the fact that $n_1+n_2+n_3+n_4=0.04$ for a Ho^{3+} concentration of 4 mol % are

$$\frac{dn_1}{dt} = -\sigma_{14}n_1\frac{I_P}{h\nu} + \frac{n_2}{\tau_2} + \frac{B_{31}}{\tau_{R_3}}n_3 - W_{\text{CR}}n_1n_4 + W_{\text{ET1}}n_2n_5 + W_{\text{ET2}}n_3n_5 + W_{\text{ETU1}}n_2^2 + W_{\text{ETU2}}n_3^2 + \frac{\beta_{41}}{\tau_{R_4}}n_4, \quad (9)$$

$$\frac{dn_2}{dt} = W_{\text{CR}}n_1n_4 + \left(\frac{B_{32}}{\tau_{R_3}} + W_{\text{nr}}(32)\right)n_3 - \frac{n_2}{\tau_2} - W_{\text{ET1}}n_2n_5 + \frac{\beta_{42}}{\tau_{R_4}}n_4 - 2W_{\text{ETU1}}n_2^2, \quad (10)$$

$$\frac{dn_3}{dt} = W_{\text{CR}}n_1n_4 - \frac{n_3}{\tau_3} - W_{\text{ET2}}n_3n_5 - 2W_{\text{ETU2}}n_3^2 + \left(\frac{\beta_{43}}{\tau_{R_4}} + W_{\text{nr}}(43)\right)n_4 + W_{\text{ETU1}}n_2^2, \quad (11)$$

$$\frac{dn_4}{dt} = \sigma_{14}n_1\frac{I_P}{h\nu} + W_{\text{ETU2}}n_3^2 - W_{\text{CR}}n_1n_4 - \frac{n_4}{\tau_4}, \quad (12)$$

where I_P is the pump intensity given in W cm^{-2} and $h\nu$ is the photon energy at 650 nm. β_{ij} represents the luminescence branching ratio and τ_{R_i} is the radiative lifetime of 5F_5 , 5I_6 and 5I_7 excited states of Ho^{3+} labeled as $i=4, 3$, and 2 , respectively.

B. Numerical simulation of the rate equation system

Calculations were performed for the singly Ho^{3+} - and the Ho^{3+} , Pr^{3+} -codoped ZBLAN glasses containing 4 mol % Ho^{3+} and 0.1, 0.2, and 0.3 mol % Pr^{3+} using a computer program incorporating the Runge-Kutta numerical method. Figure 9 shows the time evolutions of $n_2(t)$, $n_3(t)$, and $\Delta n(t)=n_3(t)-n_2(t)$, the population inversion of Ho^{3+} after switching the pump laser on at $t=0$ (using a pump rate of 80 s^{-1} at 650 nm). Equilibrium in the populations was obtained after 10 ms in the Ho^{3+} (4 mol %), Pr^{3+} (0.3 mol %)-doped ZBLAN system, see Fig. 9(b). At that stage, the value for Δn was obtained. On the other hand, equilibrium in the value for Δn in the singly Ho^{3+} -doped ZBLAN system is established at a comparatively longer time, see Fig. 9(a). In addition, $n_3 < n_2$ and $\Delta n < 0$ for most of the calculation for the singly Ho^{3+} -doped ZBLAN system.

Figure 10 shows Δn obtained for 2.92 μm laser emission from Ho^{3+} in both singly Ho^{3+} -doped and Ho^{3+} , Pr^{3+} -codoped ZBLAN systems as a function of the pump rate (R_p) for the three Pr^{3+} concentrations used in this work. The pump rates can be converted to pump intensities I_P (W/cm^2) using $I_P=(h\nu R_p)/\sigma_{\text{abs}}$, where $\sigma_{\text{abs}}({}^5I_8 \rightarrow {}^5F_5)=8.56 \times 10^{-20} \text{ cm}^2$ at 650 nm. The results presented in Fig. 10 show that 0.3 mol % Pr^{3+} , which produces a strong quenching of the 5I_7 level decay time, leads to $\Delta n > 0$. The similar Ho^{3+} (3 mol %), Pr^{3+} (0.3 mol %)-codoped ZBLAN glass has been shown experimentally to provide efficient 2.92 μm laser emission.⁹ Thus we have shown both experimentally

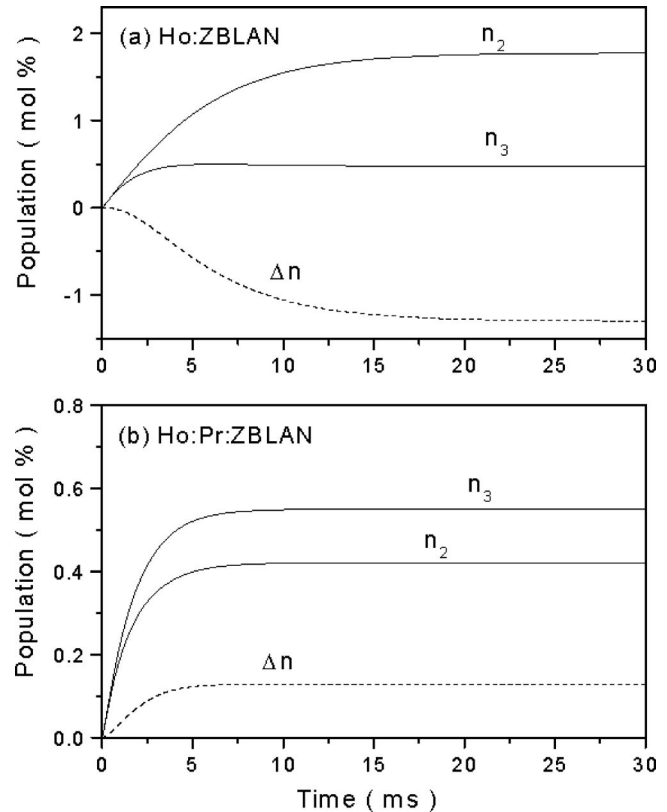


FIG. 9. Calculated evolution of the excited state populations (in mol %) of Ho^{3+} obtained by numerical simulation of the rate equations for (a) Ho^{3+} (4 mol %)-doped ZBLAN and (b) Ho^{3+} (4 mol %), Pr^{3+} (0.3 mol %)-codoped ZBLAN. The simulations were obtained under a continuous pump rate of 80 s^{-1} at 650 nm.

and theoretically that the Pr^{3+} ion is a very effective deactivator for the 2.92 μm ${}^5I_6 \rightarrow {}^5I_7$ laser transition of Ho^{3+} .

It is important to clarify that we have dealt with the total population inversion between the 5I_6 and 5I_7 multiplet levels without considering Stark splitting. We can, however, sketch out how the 5I_7 multiplet splitting will affect the calculated population inversion. The 5I_7 multiplet has three main sub-levels localized at 4835, 5049, and 5243 cm^{-1} (Ref. 15) having Boltzmann occupation factors f_i equal to 0.676, 0.234, and 0.090, respectively. For the purposes of calculating the population inversion, the 5I_6 multiplet is located at 8544 cm^{-1} with $f=1$. Three main emission lines are observed at 2.8 μm (1), 2.94 μm (2), and 3.11 μm (3). The population inversion for each ${}^5I_6 \rightarrow {}^5I_7(i)$ transition will be given by $\Delta n_i = n_3 - n_2 f_i = n_2 [(n_3/n_2) - f_i]$. In the case of Ho^{3+} (4 mol %)-doped ZBLAN, we have seen that $n_3/n_2 \ll f_3 = 0.09$, so $\Delta n_i < 0$ for all the emission lines involved in the ${}^5I_6 \rightarrow {}^5I_7$ transition. A positive but smaller population inversion can be obtained for the 2.94 and 3.11 μm emission lines in Ho^{3+} (4 mol %), Pr^{3+} (0.2 mol %)-codoped ZBLAN compared to Ho^{3+} (4 mol %), Pr^{3+} (0.3 mol %)-codoped ZBLAN.

V. CONCLUSIONS

We have investigated in detail the deactivation of the 5I_7 excited state level of Ho^{3+} in the presence of Pr^{3+} ions in ZBLAN glasses. Two energy transfer upconversion pro-

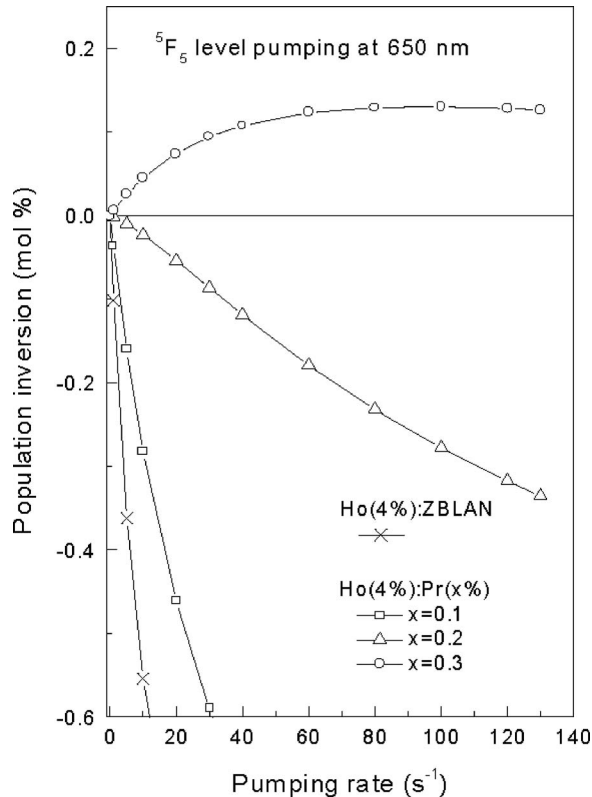


FIG. 10. Calculated population inversion (in mol %) for the laser emission at $2.9 \mu\text{m}$ obtained for a simulation with continuous laser pumping at 650 nm for (a) Ho^{3+} (4 mol %)-doped ZBLAN and (b) Ho^{3+} (4 mol %), Pr^{3+} (x mol %)-codoped ZBLAN glasses, where $x=0.1, 0.2$, and 0.3 mol %. Note that the Ho^{3+} ion concentration of 1 mol % corresponds to 1.375×10^{20} ions cm^{-3} .

cesses ETU1 and ETU2 which lead to the excitation of the 5I_6 and 5F_5 states were shown to occur in singly Ho^{3+} -doped ZBLAN glass. The rate parameters for these ETU processes were determined and it was established that the rate parameters for ETU2 were higher than those for ETU1. The rate parameter of the CR process involving the excited 5F_5 level and the 5I_8 ground state of Ho^{3+} was determined from a best fit to the 655 nm luminescence. With all the relevant energy transfer rate parameters available, we numerically solved the rate equations for the ZBLAN system under cw laser pumping at 650 nm . The results established that the Ho^{3+} (4 mol %)-doped ZBLAN glass that was codoped with 0.3 mol % Pr^{3+} showed considerable improvement in the

value of Δn as compared to the corresponding singly Ho^{3+} -doped ZBLAN glass because of strong depopulation of the 5I_7 level of Ho^{3+} by ET1. As a consequence, the doubly doped glass exhibited a maximum population inversion equal to $\sim 3.3\%$ of total Ho^{3+} population for a cw pump rate of 80 s^{-1} . These facts indicate that Ho^{3+} , Pr^{3+} -codoped ZBLAN glass is a promising candidate for high power laser operation at $2.9 \mu\text{m}$ using diode laser pumping at 650 nm . The effect of 5I_7 deactivation by Pr^{3+} ions on the population inversion of the $^5I_6 \rightarrow ^5I_7$ transition in Ho^{3+} , Pr^{3+} -codoped ZBLAN glass is comparable to the gain improvement reported for Er^{3+} , Pr^{3+} -codoped ZBLAN glass.

ACKNOWLEDGMENTS

The authors thank financial support from FAPESP (Grant Nos.1995/4166-0 and 2000/10986-0), CNPq, and the Australian Research Council.

- ¹L. D. da Vila, L. Gomes, L. V. G. Tarelho, S. J. L. Ribeiro, and Y. Messaddeq, *J. Appl. Phys.* **95**, 5451 (2004).
- ²L. D. da Vila, L. Gomes, C. R. Eyzaguirre, E. Rodriguez, C. L. César, and L. C. Barbosa, *Opt. Mater. (Amsterdam, Neth.)* **27**, 1333 (2005).
- ³J. H. Song, J. Heo, and S. H. Park, *J. Appl. Phys.* **97**, 083542 (2005).
- ⁴A. F. H. Librantz, L. Gomes, S. J. L. Ribeiro, and Y. Messaddeq, *J. Lumin.*, <http://dx.doi.org/10.1016/j.jlumin.2007.05.010>.
- ⁵A. F. H. Librantz, L. Gomes, S. J. L. Ribeiro, and Y. Messaddeq, *Proc. SPIE* **6190**, 6190G (2006).
- ⁶N. Karayianis, D. E. Wortman, and H. P. Janssen, *J. Phys. Chem. Solids* **37**, 675 (1976).
- ⁷F. H. Jagosich, L. Gomes, L. V. G. Tarelho, L. C. Courrol, and I. M. Ranieri, *J. Appl. Phys.* **91**, 624 (2002).
- ⁸S. D. Jackson, *Electron. Lett.* **39**, 772 (2003).
- ⁹S. D. Jackson, *Opt. Lett.* **29**, 334 (2004).
- ¹⁰M. Pollnau, *IEEE J. Quantum Electron.* **33**, 1982 (1997).
- ¹¹S. D. Jackson, T. A. King, and M. Pollnau, *Opt. Lett.* **24**, 1133 (1999).
- ¹²B. Srinivasan, J. Tafoya, and R. K. Jain, *Opt. Express* **4**, U10 (1999).
- ¹³X. Zhu and R. Jain, *Opt. Lett.* **32**, 26 (2007).
- ¹⁴A. I. Burshtein, *JETP Lett.* **35**, 885 (1972).
- ¹⁵L. Wetenkamp, G. F. West, and H. Többen, *J. Non-Cryst. Solids* **140**, 25 (1992).
- ¹⁶A. Braud, S. Girard, J. L. Doualan, M. Thuau, R. Moncorgé, and A. M. Tkachuk, *Phys. Rev. B* **61**, 5280 (2000).
- ¹⁷R. K. Watts, in *Optical Properties of Ions in Solids, Energy Transfer Phenomena*, edited by B. Di Bartolo (Plenum, New York, 1975), pp. 307–336.
- ¹⁸L. D. da Vila, L. Gomes, L. V. G. Tarelho, S. J. L. Ribeiro, and Y. Messaddeq, *J. Appl. Phys.* **93**, 3873 (2003).
- ¹⁹L. Gomes and F. Luty, *Phys. Rev. B* **30**, 7194 (1984).
- ²⁰J. Fernandez, R. Balda, M. L. M. Lacha, A. Oleaga, and J. L. Adam, *J. Lumin.* **94–95**, 325 (2001).
- ²¹P. S. Golding, S. D. Jackson, T. A. King, and M. Pollnau, *Phys. Rev. B* **62**, 856 (2000).